UNIVERSITEIT VAN AMSTERDAM

Bachelor Thesis Physics and Astronomy (15 EC)

Population kinetics from a two-level atomic model

By:

Sameh Mikhail

Conducted between June 2nd 2025, and August 23rd, 2025

Student number:	14003597
Research institute:	Advanced Research Center for Nanolithography
Research group:	Plasma Theory and Modeling
Supervisor:	John Sheil
Examiner:	Oscar Versolato
Faculty and university:	Faculty of Science at the University of Amsterdam

1 Abstract

This thesis investigates population kinetics in plasmas using the two-level model. The population ratio between energy levels is derived and analyzed with respect to excitation energy, electron temperature, and electron density. The results show a complex relationship between excitation energy and electron temperature, although the model converges to intuitive limits in extreme parameter regimes. The study further examines effective temperatures in non-local thermal equilibrium plasmas by comparing Hansen's[1] and Busquet's [2] formulations, showing agreement in high-density and high-temperature limits, but deviations at lower values. Additionally, the influence of the Gaunt factor on collisional-radiative rates is explored, with Mewe's [3] approximation found to yield consistently higher values than the Younger-Wiese [4] model across relevant parameter ranges. Finally, the model is extended to three levels, considering both interacting and non-interacting excited states. The non-interacting case reduces to two independent two-level systems, whereas the interacting case requires more complex coupled equations. These results demonstrate both the strengths and limitations of reduced models in capturing plasma population dynamics, providing insight for applications in astrophysics and nanolithography.

Keywords: plasma physics - Gaunt factor - population ratio - effective temperature

2 Dutch popular scientific summary

Plasma wordt vaak de vierde toestand van materie genoemd, naast vast, vloeibaar en gasvormig. Het ontstaat wanneer atomen zoveel energie krijgen dat hun elektronen losraken en er een mengsel van vrije elektronen en ionen ontstaat. Plasma speelt een centrale rol in sterren, maar komt ook dichter bij huis voor, bijvoorbeeld in bliksem, TL-lampen en de productie van computerchips.

Een belangrijk kenmerk van plasma is dat het licht kan uitzenden en absorberen. Dat gebeurt doordat elektronen tussen verschillende energieniveaus springen: als een elektron naar een hoger niveau gaat, neemt het energie op; als het terugvalt, zendt het een foton uit. Door dit licht te analyseren, kan men de eigenschappen van het plasma afleiden, zoals temperatuur en samenstelling. Dit is bijvoorbeeld onmisbaar in de sterrenkunde, maar ook in technologieën die extreem-ultraviolet licht gebruiken, zoals bij de productie van microchips.

Het beschrijven van al die sprongen is echter erg ingewikkeld, zeker wanneer een ion honderdduizenden mogelijke energieniveaus heeft. Om dit probleem hanteerbaar te maken, gebruiken natuurkundigen benaderingen. Eén van de eenvoudigste is het zogenoemde two level system, waarbij men alleen naar de overgang tussen twee energieniveaus kijkt. Ondanks zijn eenvoud geeft dit model al verrassend veel inzicht in hoe populaties van elektronen zich verdelen. In dit onderzoek is onderzocht hoe dit model afhankelijk is van de temperatuur, de dichtheid van elektronen en de energieverschillen tussen niveaus. Ook is gekeken naar correctie op dit model, zoals de zogenaamde Gaunt-factor, en hoe een uitbreiding naar drie niveaus het beeld verandert.

Door dit soort modellen te bestuderen, kunnen we beter begrijpen hoe plasma's zich gedragen - van het binnenste van een ster tot de geavanceerde laboratoria waar het licht wordt gemaakt dat onze moderne chips mogelijk maakt.

Contents

3 Introduction

Plasma is often called the fourth state of matter, alongside solid, liquid, and gas. Unlike the other three, plasma consists of a collection of freely moving charged particles: positively charged ions and negatively charged electrons. Plasmas are characterized not only by their unique collective behavior of charged particles but also by their ability to emit and absorb radiation. This radiation arises from a variety of processes, such as electron-ion collisions, recombination, and transitions between discrete atomic or ionic energy states. Understanding these radiative mechanisms is essential for both diagnosing plasma conditions in laboratory and astrophysical environments and for designing practical applications, such as fusion devices or plasma-based light sources [5].

A particularly important application of these radiative mechanisms lies in astrophysics, where the concept of population dynamics of energy levels plays a crucial role. One approach is to interpret results based on average plasma properties, but this way the detailed information about the plasma is lost or it might lead to wrong results. For instance, when trying to measure the composition of the plasma under coronal conditions, by looking at the spectrum of the plasma, one must take into account that for a plasma with several ions having an atomic number ranging between 6 and 28. The relevant transitions mainly belong to the H-like, He-like, Li-like, and Ne-like sequences. For these cases, detailed quantum-mechanical calculations are often impractical, so simple interpolation formulae are required. Such formulae allow one to estimate electron-impact excitation cross sections and rate coefficients with sufficient accuracy for astrophysical applications [3].

Another field where the population dynamics of plasma energy levels is of central importance is in the generation of extreme ultraviolet (EUV) light, such as in advanced nanolithography systems. In these devices, high-intensity laser pulses are focused on microscopic tin droplets to create a hot, dense plasma that emits radiation around 13.5 nm. To optimize the efficiency of EUV light production, it is crucial to understand and predict how electrons in the plasma excite and ionize the various charge states of tin. As in astrophysical plasmas, relying solely on average properties is insufficient, since the emitted spectrum depends sensitively on the population distribution across multiple ionization stages. Detailed quantum-mechanical calculations of excitation cross sections for these highly charged ions are computationally demanding, so practical approaches often involve simplified models and interpolation formulae that still capture the relevant physics with sufficient accuracy [6].

The calculation of population of energy levels in plasmas is thus a crucial aspect of quantifying the radiation produced by a plasma. The population flow is described using the following equation,

$$\frac{\mathrm{d}n_i}{\mathrm{d}t} = \sum_p \sum_{k \neq i} n_k \mathcal{R}^p_{ki} - n_i \sum_p \sum_{k \neq i} \mathcal{R}^p_{ik} \tag{1}$$

where n_i is the population density of level i, $\mathcal{R}^p_{ki}$ is the rate of transition from level k to level i for process p, and the sums run over all processes p and all populations k that are not equal to i. The equation states that the change in population density is determined by the difference between the inflow of atoms that are transitioning from a level k into level i, which happens with a rate $\mathcal{R}^p_{ki}$ and the outflow of atoms that are transitioning from level i to a level k, which happens with a rate $\mathcal{R}^p_{ik}$.

The problem, however, is that the number of energy levels per ion can be enormous, leading to a huge system of ordinary differential equations (ODEs) that describe the population dynamics of these levels. For ions having over 10^6 energy levels, this is computationally not feasible [7].

To be able to solve this problem, one must use approximations to reduce the complexity of the system. One such approximation is to use so-called effective temperatures, which can be

calculated using a simple two-level model. In Sheil et al. [7], the authors show the validity of this two-level model and provide the equation describing the two-level model,

$$\frac{n_2}{n_1} = \frac{g_2}{g_1} \exp\left\{-\frac{E_{21}}{T_\mathrm{e}}\right\} \left(1 + \frac{\mathcal{C} E_{21}^3 T_e^{1/2}}{n_e \bar{g}}\right)^{-1} \tag{2}$$

where n_1 and n_2 are the populations of the two energy levels, and the ratio describes the population distribution between the two levels. Here, there are four important quantities: the excitation energy E_{21}, the plasma temperature T_e (specifically the electron temperature), the electron density n_e, and the Gaunt factor $\bar{g}$.

The goal of this thesis is to study the two-level model. This will be done by first deriving the equation for the two-level model to understand where it comes from, After which we will look at how the population depends on the key parameters. Then, we will make the connection between the equation for the two-level model and the effective temperatures. After that, we will look into a factor that influences the population dynamics, the so-called Gaunt factor $\bar{g}$. Finally, we will try to add more complexity to the model by including an additional energy level and their interactions.

4 Theory

4.1 Population flow in two-level system

To evaluate equation 1, one must first understand the atomic processes in hot plasma. The processes can be placed into different categories. There are two spontaneous processes [8] (meaning that they happen without any external influence):

- $\mathcal{R}^{\mathrm{se}}$: spontaneous emission (se) - the excited ion emits a photon and goes into a lower energy state. The energy difference between the two states is carried away by the photon.
- $\mathcal{R}^{\mathrm{ai}}$: autoionization (ai) - an excited ion (where the energy level lies above the ionization potential) makes a transition where one electron decays to a lower energy state, while the other electron is ejected, thus the original ion is ionized.

and six electron-ion processes [8]:

- $\mathcal{R}^{\mathrm{ci}}$: electron-impact ionization (ci) - an electron collides with the ion and provides enough energy to remove a bound electron, ionizing the ion.
- $\mathcal{R}^{\mathrm{tbr}}$: three-body recombination (tbr) - two electrons are near an ion, and one of them is captured by the ion, while the other electron carries away the excess energy.
- $\mathcal{R}^{\mathrm{rr}}$: radiative recombination (rr) - an electron is captured by an ion, and a photon is emitted in the process.
- $\mathcal{R}^{\mathrm{dc}}$: dielectronic capture (dc) - an electron is captured by an ion, and the released energy is used to excite a bound electron to a higher energy state, creating a doubly excited ion.
- $\mathcal{R}^{\mathrm{ce}}$: electron-impact excitation (ce) - a free electron near the ion loses energy, exciting the bound electron to a higher energy state (while the free electron remains free).
- $\mathcal{R}^{\mathrm{de}}$: electron-impact de-excitation (de) - a free electron near the ion gains energy, de-exciting the bound electron to a lower energy state (while the free electron remains free).

which are dominant in the absence of external radiation fields.

One can see the table below to have an overview of the above given processes [9].

p	Name	Description	p	Name	Description
$\mathcal{R}^{\mathrm{se}}$	spontaneous emission	$A^* \to A + \gamma$	-	-	-
$\mathcal{R}^{\mathrm{ce}}$	electron-impact excitation	$A + e \to A^* + e$	$\mathcal{R}^{\mathrm{de}}$	electron-impact de-excitation	$A^* + e \to A + e$
$\mathcal{R}^{\mathrm{ai}}$	autoionization	$A^* \to A^{**} + e$	$\mathcal{R}^{\mathrm{dc}}$	dielectronic capture	$A^{**} + e \to A^*$
$\mathcal{R}^{\mathrm{ci}}$	electron-impact ionization	$A + e \to A^{**} + e + e$	$\mathcal{R}^{\mathrm{tbr}}$	three-body recombination	$A^{**} + e + e \to A + e$
-	-	-	$\mathcal{R}^{\mathrm{rr}}$	radiative recombination	$A^{**} + e \to A + \gamma$

Table 1: Overview of the processes and their rates. The set of a direct process with its reverse/indirect process is called a balanced process. A^* and A^{**} denote the excited and doubly excited states respectively.

Visual representation of these processes is given below:

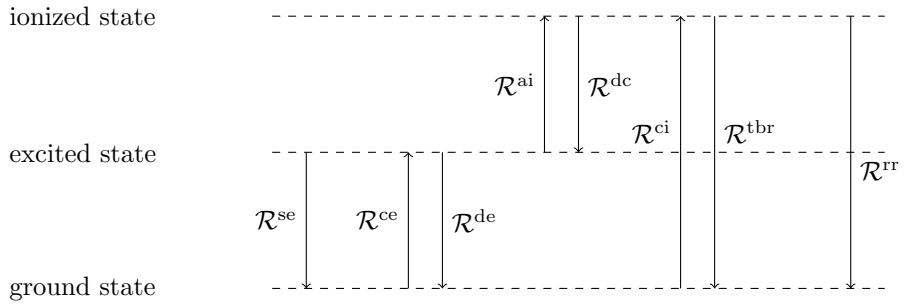

Considering the processes between the ground state and excited state, the rate equation (Eq. 1) for the two-level system becomes,

$$\frac{\mathrm{d}n_2}{\mathrm{d}t} = n_1\mathcal{R}_{12}^{\mathrm{ce}} - n_2(\mathcal{R}_{21}^{\mathrm{se}} + \mathcal{R}_{21}^{\mathrm{de}}) \tag{3}$$

for the two-level system. For plasmas the local thermal equilibrium is reached under the following conditions:

- The population density does not change over time, which is called the steady state, $\dfrac{\mathrm{d}n_i}{\mathrm{d}t} = 0$.
- The radiative processes are negligible compared to the collisional processes.
- The population density can be described using Boltzmann's law, $n_i \propto g_i \exp\left\{-\frac{E_i}{k_B T_{\mathrm{e}}}\right\}$ [10].

Therefore, for the steady state system, Eq. 3 can be rewritten as,

$$\frac{n_2}{n_1} = \frac{\mathcal{R}_{12}^{\mathrm{ce}}}{\mathcal{R}_{21}^{\mathrm{se}} + \mathcal{R}_{21}^{\mathrm{de}}} \tag{4}$$

and using the principle of detailed balance [11], which states that the population flux of collisional excitation must equal the population flux of collisional de-excitation (this only holds in thermal equilibrium),

$$n_1\mathcal{R}_{12}^{\mathrm{ce}} = n_2\mathcal{R}_{21}^{\mathrm{de}} \longrightarrow \mathcal{R}_{12}^{\mathrm{ce}} = \frac{n_2}{n_1}\mathcal{R}_{21}^{\mathrm{de}} \tag{5}$$

equation 4 becomes,

$$\frac{n_2}{n_1} = \left[\frac{n_1}{n_2}\right]^{-1} = \left[\frac{\mathcal{R}_{21}^{\mathrm{se}} + \mathcal{R}_{21}^{\mathrm{de}}}{\mathcal{R}_{12}^{\mathrm{ce}}}\right]^{-1} = \left[\frac{\mathcal{R}_{21}^{\mathrm{se}} + \mathcal{R}_{21}^{\mathrm{de}}}{\frac{n_2}{n_1}\mathcal{R}_{21}^{\mathrm{de}}}\right]^{-1} = \left[\frac{n_1}{n_2}\left(1 + \frac{\mathcal{R}_{21}^{\mathrm{se}}}{\mathcal{R}_{21}^{\mathrm{de}}}\right)\right]^{-1} \tag{6}$$

The expressions for the rates are given by [12],

$$\mathcal{R}_{21}^{\mathrm{se}} = \mathcal{C}^{\mathrm{se}} f_{21} E_{21}^2 \qquad \text{with} \qquad \mathcal{C}^{\mathrm{se}} = 4.3 \times 10^7 \ \mathrm{eV}^{-2}\ \mathrm{s}^{-1} \tag{7}$$

$$\mathcal{R}_{21}^{\mathrm{de}} = \mathcal{C}^{\mathrm{de}} \frac{n_e f_{21} \bar{g}}{E_{21}\sqrt{k_B T_e}} \qquad \text{with} \qquad \mathcal{C}^{\mathrm{de}} = 1.6 \times 10^{-5} \ \mathrm{eV}^{3/2}\ \mathrm{cm}^3\ \mathrm{s}^{-1} \tag{8}$$

where the energy difference $E_{21} \equiv E_2 - E_1$ is given in terms of eV, temperature T_e in K, and the electron density n_e in cm^{-3}. The oscillator strength f_{21} is a dimensionless parameter that describes the probability of a transition between two energy levels [13], and $\bar{g}$ the Gaunt factor (more of that in section 4.4). Using Boltzmann law and Eqs. 7 and 8 in Eq. 6,

$$\begin{aligned}
\frac{n_2}{n_1} &= \frac{n_2}{n_1}\left(1 + \frac{\mathcal{C}^{\mathrm{se}}}{\mathcal{C}^{\mathrm{de}}}\frac{f_{21}E_{21}^2}{\frac{n_e f_{21}\bar{g}}{E_{21}\sqrt{k_B T_e}}}\right)^{-1} \\
&= \frac{g_2 \exp\left\{-\frac{E_2}{k_B T_\mathrm{e}}\right\}}{g_1 \exp\left\{-\frac{E_1}{k_B T_\mathrm{e}}\right\}}\left(1 + \frac{\mathcal{C}^{\mathrm{se}}}{\mathcal{C}^{\mathrm{de}}}\frac{E_{21}^3\sqrt{k_B T_e}}{n_e\bar{g}}\right)^{-1} \\
&= \frac{g_2}{g_1}\exp\left\{-\frac{E_{21}}{k_B T_\mathrm{e}}\right\}\left(1 + \frac{\mathcal{C}E_{21}^3(k_B T_e)^{1/2}}{n_e\bar{g}}\right)^{-1}
\end{aligned} \tag{9}$$

where $\mathcal{C} = \mathcal{C}^{\mathrm{se}}/\mathcal{C}^{\mathrm{de}} = 2.69\times10^{12}\ \mathrm{eV}^{-7/2}\ \mathrm{cm}^{-3}$, Eq. 9 gives the population density ratio for a two-level system. As the temperature is measured in electronvolts, the expression can be simplified to [7]:

$$\boxed{\frac{n_2}{n_1} = \frac{g_2}{g_1}\exp\left\{-\frac{E_{21}}{T_\mathrm{e}}\right\}\left(1 + \frac{\mathcal{C}E_{21}^3 T_e^{1/2}}{n_e\bar{g}}\right)^{-1}} \tag{10}$$

4.2 Impact of key parameters on population distribution

In the equation regarding the reduced population density ratio of a two-level system,

$$\frac{n_2 g_2^{-1}}{n_1 g_1^{-1}} = \exp\left\{-\frac{E_{21}}{T_\mathrm{e}}\right\}\left(1+\frac{\mathcal{C}E_{21}^3 T_e^{1/2}}{n_e \bar{g}}\right)^{-1} \tag{11}$$

there are three parameters that can be varied:

- T_e: the true electron temperature, which is based on the kinetic energy of the electrons in the plasma and is defined as which is the temperature in local thermal equilibrium.
- n_e: the electron density, which is the number of electrons per unit volume.
- E_{21}: the energy difference between the two energy levels, which is a property of the ion and does not change in the plasma.

Considering the cases for the parameters as in Sheil's paper [7]:

- $T_\mathrm{e} = 45$ eV, corresponding to a temperature of $T_\mathrm{e} = 5.2 \times 10^5$ K (using the Boltzmann factor to go from electronvolt to Kelvin).
- $E_{21} = 75$ eV, which is the energy difference between the ground state and the first excited state for the following transitions

$$E_{4p^5 4d} - E_{4p^6} \approx E_{4p^4 4d^2} - E_{4p^5 4d} \approx E_{4p^3 4d^3} - E_{4p^4 4d^2} \approx 75 \text{ eV} \tag{12}$$

- $n_e = 10^{19} - 10^{21}$ cm^{-3}, based on the three presented cases in the paper.

These are the values that are used as anchors in the following analysis. To analyze the impact of the parameters, we examine the relationship between the reduced population density ratio and the parameters, considering the limits as the parameters approach zero and infinity, and by evaluating the derivatives with respect to the parameters to determine how the ratio responds to changes.

4.2.1 Impact of electron density

The relation between the electron density n_e and the ratio of the reduced population ratio is given by,

$$\frac{n_2 g_2^{-1}}{n_1 g_1^{-1}} \propto \left(1+\frac{1}{n_e}\right)^{-1} \tag{13}$$

and to see how the reduced population density ratio behaves at the extremes, take the limits,

$$\lim_{n_e\to 0}\frac{n_2 g_2^{-1}}{n_1 g_1^{-1}} = \exp\left\{-\frac{E_{21}}{T_\mathrm{e}}\right\}\lim_{n_e\to 0}\left(1+\frac{\mathcal{C}E_{21}^3 T_e^{1/2}}{n_e \bar{g}}\right)^{-1} = 0 \tag{14}$$

$$\lim_{n_e\to \infty}\frac{n_2 g_2^{-1}}{n_1 g_1^{-1}} = \exp\left\{-\frac{E_{21}}{T_\mathrm{e}}\right\}\lim_{n_e\to \infty}\left(1+\frac{\mathcal{C}E_{21}^3 T_e^{1/2}}{n_e \bar{g}}\right)^{-1} = \exp\left\{-\frac{E_{21}}{T_\mathrm{e}}\right\} \tag{15}$$

so the reduced population ratio converges to zero for very low electron density and converges to the Boltzmann factor for very high electron density. This is expected, since there might be higher levels but not enough electrons to populate, so the reduced population ratio is zero. For very high

electron densities the collisions between electrons and ions increases, leading to a local thermal equilibrium which is governed by the Boltzmann distribution. When taking the derivative of Eq. 11 with respect to the electron density,

$$\begin{aligned}
\frac{\partial}{\partial n_e}\left[\frac{n_2 g_2^{-1}}{n_1 g_1^{-1}}\right] &= \frac{\partial}{\partial n_e}\left[\exp\left\{-\frac{E_{21}}{T_\mathrm{e}}\right\}\left(1+\frac{\mathcal{C}E_{21}^3 T_e^{1/2}}{n_e\bar{g}}\right)^{-1}\right] \\
&= \exp\left\{-\frac{E_{21}}{T_\mathrm{e}}\right\}\frac{\partial}{\partial n_e}\left[\left(1+\frac{\mathcal{C}E_{21}^3 T_e^{1/2}}{n_e\bar{g}}\right)^{-1}\right] \\
&= -\exp\left\{-\frac{E_{21}}{T_\mathrm{e}}\right\}\left(1+\frac{\mathcal{C}E_{21}^3 T_e^{1/2}}{n_e\bar{g}}\right)^{-2}\frac{\partial}{\partial n_e}\left[\left(1+\frac{\mathcal{C}E_{21}^3 T_e^{1/2}}{n_e\bar{g}}\right)\right] \\
&= -\exp\left\{-\frac{E_{21}}{T_\mathrm{e}}\right\}\left(1+\frac{\mathcal{C}E_{21}^3 T_e^{1/2}}{n_e\bar{g}}\right)^{-2}\left(-\frac{\mathcal{C}E_{21}^3 T_e^{1/2}}{n_e^2\bar{g}}\right) \\
&= \left(\frac{n_e\bar{g}}{n_e\bar{g}+\mathcal{C}E_{21}^3 T_e^{1/2}}\right)^2\left(\frac{\mathcal{C}E_{21}^3 T_e^{1/2}}{n_e^2\bar{g}}\right)\exp\left\{-\frac{E_{21}}{T_\mathrm{e}}\right\} \\
&= \frac{\mathcal{C}\bar{g}E_{21}^3 T_e^{1/2}}{\left(n_e\bar{g}+\mathcal{C}E_{21}^3 T_e^{1/2}\right)^2}\exp\left\{-\frac{E_{21}}{T_\mathrm{e}}\right\}
\end{aligned} \tag{16}$$

It shows that the reduced population ratio has no maximum or minimum with respect to the electron density, since its derivative with respect to electron density is always positive. At very high electron densities, the derivative approaches zero, and the reduced population ratio converges to the Boltzmann factor.

4.2.2 Impact of excitation energy

The relation between the energy difference E_{21} and the ratio of the reduced population density is given by,

$$\frac{n_2 g_2^{-1}}{n_1 g_1^{-1}} \propto \exp\left\{-E_{21}\right\}\left(1+E_{21}^3\right)^{-1} \tag{17}$$

and to examine the behavior of the reduced population density ratio in the limiting cases, we evaluate its limits,

$$\lim_{E_{21}\to 0}\frac{n_2 g_2^{-1}}{n_1 g_1^{-1}} = \lim_{E_{21}\to 0}\exp\left\{-\frac{E_{21}}{T_\mathrm{e}}\right\}\left(1+\frac{\mathcal{C}E_{21}^3 T_e^{1/2}}{n_e\bar{g}}\right)^{-1} = 1 \tag{18}$$

$$\lim_{E_{21}\to \infty}\frac{n_2 g_2^{-1}}{n_1 g_1^{-1}} = \lim_{E_{21}\to \infty}\exp\left\{-\frac{E_{21}}{T_\mathrm{e}}\right\}\left(1+\frac{\mathcal{C}E_{21}^3 T_e^{1/2}}{n_e\bar{g}}\right)^{-1} = 0 \tag{19}$$

which shows that if there is no energy difference between the two levels, they are equally populated and the reduced population ratio equals one. When the energy difference is very large, the ratio approaches zero, since the higher level can no longer be populated. When taking the

derivative with respect to the energy difference,

$$\begin{aligned}
\frac{\partial}{\partial E_{21}}\left[\frac{n_2 g_2^{-1}}{n_1 g_1^{-1}}\right] &= \frac{\partial}{\partial E_{21}}\left[\exp\left\{-\frac{E_{21}}{T_\mathrm{e}}\right\}\left(1+\frac{\mathcal{C}E_{21}^3 T_e^{1/2}}{n_e\bar{g}}\right)^{-1}\right] \\
&= \frac{\partial}{\partial E_{21}}\left[\exp\left\{-\frac{E_{21}}{T_\mathrm{e}}\right\}\right]\left(1+\frac{\mathcal{C}E_{21}^3 T_e^{1/2}}{n_e\bar{g}}\right)^{-1} \\
&\quad + \exp\left\{-\frac{E_{21}}{T_\mathrm{e}}\right\}\frac{\partial}{\partial E_{21}}\left[\left(1+\frac{\mathcal{C}E_{21}^3 T_e^{1/2}}{n_e\bar{g}}\right)^{-1}\right] \\
&= -\frac{1}{T_\mathrm{e}}\exp\left\{-\frac{E_{21}}{T_\mathrm{e}}\right\}\left(1+\frac{\mathcal{C}E_{21}^3 T_e^{1/2}}{n_e\bar{g}}\right)^{-1} \\
&\quad - \exp\left\{-\frac{E_{21}}{T_\mathrm{e}}\right\}\left(1+\frac{\mathcal{C}E_{21}^3 T_e^{1/2}}{n_e\bar{g}}\right)^{-2}\frac{\partial}{\partial E_{21}}\left[1+\frac{\mathcal{C}E_{21}^3 T_e^{1/2}}{n_e\bar{g}}\right] \\
&= -\frac{1}{T_\mathrm{e}}\exp\left\{-\frac{E_{21}}{T_\mathrm{e}}\right\}\left(1+\frac{\mathcal{C}E_{21}^3 T_e^{1/2}}{n_e\bar{g}}\right)^{-1} \\
&\quad - \exp\left\{-\frac{E_{21}}{T_\mathrm{e}}\right\}\left(1+\frac{\mathcal{C}E_{21}^3 T_e^{1/2}}{n_e\bar{g}}\right)^{-2}\left(\frac{3\mathcal{C}E_{21}^2 T_e^{1/2}}{n_e\bar{g}}\right) \\
&= -\left(\frac{n_e\bar{g}}{T_e}\frac{n_e\bar{g}+\mathcal{C}E_{21}^3 T_e^{1/2}+3\mathcal{C}E_{21}^2 T_e^{3/2}}{\left(n_e\bar{g}+\mathcal{C}E_{21}^3 T_e^{1/2}\right)^2}\right)\exp\left\{-\frac{E_{21}}{T_\mathrm{e}}\right\}
\end{aligned} \tag{20}$$

It shows that the reduced population ratio decreases monotonically with increasing energy difference, starting below zero and approaching zero asymptotically at very large energy differences. Since the derivative is always negative, the function has no maxima or minima with respect to the energy difference.

4.2.3 Impact of electron temperature

The relation between the electron temperature T_e and the ratio of the reduced population density is given by,

$$\frac{n_2 g_2^{-1}}{n_1 g_1^{-1}} \propto \exp\left\{-\frac{1}{T_\mathrm{e}}\right\}\left(1+T_\mathrm{e}^{3/2}\right)^{-1} \tag{21}$$

and to see how the reduced population density ratio behaves at the extremes, take the limits,

$$\lim_{T_\mathrm{e}\to 0}\frac{n_2 g_2^{-1}}{n_1 g_1^{-1}} = \lim_{T_\mathrm{e}\to 0}\exp\left\{-\frac{E_{21}}{T_\mathrm{e}}\right\}\left(1+\frac{\mathcal{C}E_{21}^3 T_e^{1/2}}{n_e\bar{g}}\right)^{-1} = 0 \tag{22}$$

$$\lim_{T_\mathrm{e}\to \infty}\frac{n_2 g_2^{-1}}{n_1 g_1^{-1}} = \lim_{T_\mathrm{e}\to \infty}\exp\left\{-\frac{E_{21}}{T_\mathrm{e}}\right\}\left(1+\frac{\mathcal{C}E_{21}^3 T_e^{1/2}}{n_e\bar{g}}\right)^{-1} = 0 \tag{23}$$

which means that the reduced population ratio converges to zero for very low and very high electron temperatures. This is expected, since for very low electron temperatures the electrons

do not have enough energy to populate the second level, and for very high electron temperatures the electrons are so energetic that they overcome the coulomb potential barrier and ionize the ion, leaving both levels unpopulated. When taking the derivative with respect to the electron temperature,

$$\begin{aligned}
\frac{\partial}{\partial T_\mathrm{e}}\left[\frac{n_2 g_2^{-1}}{n_1 g_1^{-1}}\right] &= \frac{\partial}{\partial T_\mathrm{e}}\left[\exp\left\{-\frac{E_{21}}{T_\mathrm{e}}\right\}\left(1+\frac{\mathcal{C}E_{21}^3 T_e^{1/2}}{n_e\bar{g}}\right)^{-1}\right] \\
&= \frac{\partial}{\partial T_\mathrm{e}}\left[\exp\left\{-\frac{E_{21}}{T_\mathrm{e}}\right\}\right]\left(1+\frac{\mathcal{C}E_{21}^3 T_e^{1/2}}{n_e\bar{g}}\right)^{-1} \\
&\quad + \exp\left\{-\frac{E_{21}}{T_\mathrm{e}}\right\}\frac{\partial}{\partial T_\mathrm{e}}\left[\left(1+\frac{\mathcal{C}E_{21}^3 T_e^{1/2}}{n_e\bar{g}}\right)^{-1}\right] \\
&= \frac{E_{21}}{T_\mathrm{e}^2}\exp\left\{-\frac{E_{21}}{T_\mathrm{e}}\right\}\left(1+\frac{\mathcal{C}E_{21}^3 T_e^{1/2}}{n_e\bar{g}}\right)^{-1} \\
&\quad - \exp\left\{-\frac{E_{21}}{T_\mathrm{e}}\right\}\left(1+\frac{\mathcal{C}E_{21}^3 T_e^{1/2}}{n_e\bar{g}}\right)^{-2}\frac{\partial}{\partial T_\mathrm{e}}\left[1+\frac{\mathcal{C}E_{21}^3 T_e^{1/2}}{n_e\bar{g}}\right] \\
&= \left[\frac{E_{21}}{T_\mathrm{e}^2}\left(1+\frac{\mathcal{C}E_{21}^3 T_e^{1/2}}{n_e\bar{g}}\right)^{-1}\right. \\
&\qquad \left. -\frac{\mathcal{C}E_{21}^3}{2n_e\bar{g}T_e^{1/2}}\left(1+\frac{\mathcal{C}E_{21}^3 T_e^{1/2}}{n_e\bar{g}}\right)^{-2}\right]\exp\left\{-\frac{E_{21}}{T_\mathrm{e}}\right\}
\end{aligned} \tag{24}$$

and setting the derivative to zero,

$$\begin{aligned}
\frac{E_{21}}{T_\mathrm{e}^2}\left(1+\frac{\mathcal{C}E_{21}^3 T_e^{1/2}}{n_e\bar{g}}\right)^{-1} - \frac{\mathcal{C}E_{21}^3}{2n_e\bar{g}T_e^{1/2}}\left(1+\frac{\mathcal{C}E_{21}^3 T_e^{1/2}}{n_e\bar{g}}\right)^{-2} &= 0 \\
E_{21}\left(1+\frac{\mathcal{C}E_{21}^3 T_e^{1/2}}{n_e\bar{g}}\right) - \frac{\mathcal{C}E_{21}^3 T_e^{3/2}}{2n_e\bar{g}} &= 0
\end{aligned} \tag{25}$$

Using u substitution, the equation can be rewritten as,

$$\begin{aligned}
au^3 - 2au - E_{21} = 0 \qquad u = T_\mathrm{e}^{1/2} \qquad a = \frac{\mathcal{C}E_{21}^3}{2n_e\bar{g}} \\
u^3 - 2u - \frac{E_{21}}{a} = 0
\end{aligned} \tag{26}$$

which can be solved using Cardano's method for solving cubic equations,

$$y^3 + py + q = 0 \qquad \rightarrow \qquad y = \sqrt[3]{-\frac{q}{2}+\sqrt{\left(\frac{q}{2}\right)^2+\left(\frac{p}{3}\right)^3}} + \sqrt[3]{-\frac{q}{2}-\sqrt{\left(\frac{q}{2}\right)^2+\left(\frac{p}{3}\right)^3}} \tag{27}$$

for the case of $p=-2$ and $q=-\frac{E_{21}}{a}$, the solution is:

$$u = \sqrt[3]{\frac{E_{21}}{2a}+\sqrt{\left(-\frac{E_{21}}{2a}\right)^2+\left(-\frac{2}{3}\right)^3}} + \sqrt[3]{\frac{E_{21}}{2a}-\sqrt{\left(-\frac{E_{21}}{2a}\right)^2+\left(-\frac{2}{3}\right)^3}} \tag{28}$$

4.3 Effective temperature in hot plasmas

The notion of temperature is a fundamental concept in describing the state of hot plasmas. In the previous sections, the temperature was defined based on LTE which assumes the Boltzmann distribution. In practice, however, the populations are often not in thermal equilibrium [14]. Fournier et al. shows that there is evidence for a temperature law in non-LTE hot plasmas [15], namely a Boltzmann law at some effective temperature T_{eff}, smaller than the electron temperature T_e [16]. Understanding the effective temperature is key to describe the population distribution in such cases.

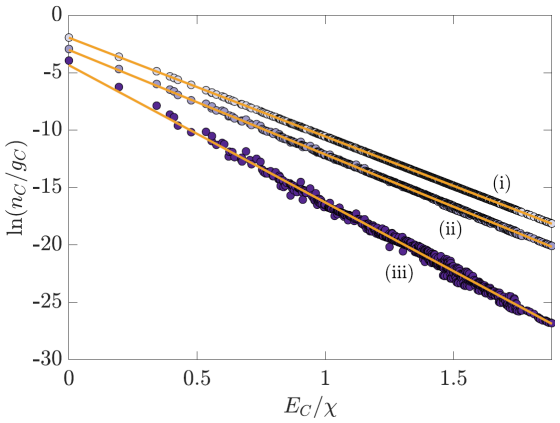

Figure 1: Reduced populations $\ln(n_C/g_C)$ as a function of the energy configuration E_C over the ionization potential χ, including a fit showing that the population shows a trend that can be described using an effective temperature in the form of the Boltzmann's law (with now T_{eff} in the place of T_e). The plot is taken from Sheil et al. [7].

4.3.1 Hansen's effective temperature

Suppose that the ratio of the reduced populations is governed by an effective temperature,

$$\frac{n_2 g_2^{-1}}{n_1 g_1^{-1}} = \exp\left\{-\frac{E_{21}}{T_{\text{eff}}}\right\} = \left(1 + \frac{\mathcal{R}_{21}^{\text{se}}}{\mathcal{R}_{21}^{\text{de}}}\right)^{-1} \tag{29}$$

using the expression for the population density ratio of a two-level system [7],

$$\frac{n_2}{n_1} = \frac{g_2}{g_1} \exp\left\{-\frac{E_{21}}{T_{\text{e}}}\right\} \left(1 + \frac{\mathcal{C} E_{21}^3 T_e^{1/2}}{n_e \bar{g}}\right)^{-1} \tag{30}$$

and recalling the expressions for the radiative rates [12],

$$\mathcal{R}_{21}^{\text{se}} = 4.3 \times 10^7 f_{21} E_{21}^2 \tag{31}$$

$$\mathcal{R}_{21}^{\text{de}} = 1.6 \times 10^{-5} \frac{n_e f_{21} \bar{g}}{E_{21} \sqrt{T_e}} \tag{32}$$

derive the effective temperature by using the ratio of the population densities,

$$\begin{aligned}\exp\left\{-\frac{E_{21}}{T_{\rm eff}}\right\} &= \frac{n_2 g_2^{-1}}{n_1 g_1^{-1}} \\ &= \exp\left\{-\frac{E_{21}}{T_{\rm e}}\right\}\left(1+\frac{\mathcal{C}E_{21}^3 T_e^{1/2}}{n_e\bar{g}}\right)^{-1} \\ -\frac{E_{21}}{T_{\rm eff}} &= -\frac{E_{21}}{T_{\rm e}} + \ln\left(\left[1+\frac{\mathcal{C}E_{21}^3 T_e^{1/2}}{n_e\bar{g}}\right]^{-1}\right)\end{aligned} \tag{33}$$

results in the expression for the effective temperature,

$$\boxed{\frac{1}{T_{\rm eff}} = \frac{1}{T_{\rm e}} + \frac{1}{E_{21}}\ln\left(1+\frac{\mathcal{C}E_{21}^3 T_e^{1/2}}{n_e\bar{g}}\right)} \tag{34}$$

which is somewhat similar to the expression for the effective temperature [1] derived by Hansen et al. in 2006 with two different aspects:

- The used expression for the Gaunt factor $\bar{g}$ is the one with $\Delta n \neq 0$.
- The constant in the paper is $\mathcal{C} = 2.75 \times 10^{12}$ eV$^{-7/2}$ cm^{-3}.

4.3.2 Busquet's effective temperature

Comparing Eq. 34 to the paper by Busquet [2] who defines the inverse of the effective temperature by the negative derivative of the population density ratio with respect to the excitation energy,

$$\begin{aligned}\frac{1}{T_{\rm eff,\,B}} &\equiv -\frac{\partial}{\partial E_{21}}\left[\ln\left(\frac{n_2 g_2^{-1}}{n_1 g_1^{-1}}\right)\right] = -\frac{\partial}{\partial E_{21}}\left[\ln\left(\exp\left\{-\frac{E_{21}}{T_{\rm e}}\right\}\left(1+\frac{\mathcal{C}E_{21}^3 T_e^{1/2}}{n_e\bar{g}}\right)^{-1}\right)\right] \\ &= -\frac{\partial}{\partial E_{21}}\left[\ln\left(\exp\left\{-\frac{E_{21}}{T_{\rm e}}\right\}\right)\right] - \frac{\partial}{\partial E_{21}}\left[\ln\left(\left(1+\frac{\mathcal{C}E_{21}^3 T_e^{1/2}}{n_e\bar{g}}\right)^{-1}\right)\right] \\ &= -\frac{\partial}{\partial E_{21}}\left[-\frac{E_{21}}{T_{\rm e}}\right] + \frac{\partial}{\partial E_{21}}\left[\ln\left(1+\frac{\mathcal{C}E_{21}^3 T_e^{1/2}}{n_e\bar{g}}\right)\right] \\ &= \frac{1}{T_{\rm e}} + \frac{3\mathcal{C}E_{21}^2 T_e^{1/2}}{n_e\bar{g}}\left(1+\frac{\mathcal{C}E_{21}^3 T_e^{1/2}}{n_e\bar{g}}\right)^{-1} = \frac{1}{T_{\rm e}} + \frac{3\mathcal{C}E_{21}^2 T_e^{1/2}}{n_e\bar{g}}\left(\frac{n_e\bar{g}}{\mathcal{C}E_{21}^3 T_e^{1/2}+n_e\bar{g}}\right) \\ &= \frac{1}{T_{\rm e}} + \frac{3\mathcal{C}E_{21}^2 T_e^{1/2}}{\mathcal{C}E_{21}^3 T_e^{1/2}+n_e\bar{g}} = \boxed{\frac{1}{T_{\rm e}} + \frac{3}{E_{21}}\left(1+\frac{n_e\bar{g}}{\mathcal{C}E_{21}^3 T_e^{1/2}}\right)^{-1}}\end{aligned} \tag{35}$$

This is also used in [7]. By taking the difference of both effective temperatures,

$$|T_{\rm eff} - T_{\rm eff,\,B}| = \frac{1}{E_{21}}\left|\ln\left(1+\frac{\mathcal{C}E_{21}^3 T_e^{1/2}}{n_e\bar{g}}\right) - 3\left(1+\frac{n_e\bar{g}}{\mathcal{C}E_{21}^3 T_e^{1/2}}\right)^{-1}\right| \tag{36}$$

one can show the difference in behaviour of both descriptions of the effective temperature.

4.4 Influence of Gaunt factor on the population ratio

In section 4.1, where the population ratio of a two level system was derived, the effective Gaunt factor $\bar{g}$ was introduced as a dimensionless parameter. The formally known bound-bound Gaunt factor was introduced to account for the influence of the quantum mechanical effects on the oscillator strength [8]. The oscillator strength is related to the strength of the absorption spectrum of an element, which is relevant to the cross section of the excitation process.

To calculate the population ratio, one needs to consider the radiative transition rates, which can be calculated by integrating the product of the cross-section and the electron velocity over a Maxwellian distribution,

$$\mathcal{R}_{ij} = \sqrt{\frac{8T_e}{\pi m_e}} y^2 \int_1^\infty Q_{ij} e^{-yU} U dU \tag{37}$$

where $y = E_{ij}/T_e$ is the ratio of the energy difference between the two levels and the electron temperature, both in eV, $U = E/E_{ij}$ is the ratio of the energy of the impinging electron to the transition energy [3], and T_e and m_e are the electron temperature and mass, respectively.

The cross section Q_{ij}, measures the probability of a process occurring from state i to state j. There are different approximations - which are based on asymptotic behaviour - that try to describe the cross section for exciting an ion, like the Bethe approximation, [17]

$$\sigma_{ij}(E_i) = \frac{8\pi}{\sqrt{3}} \frac{1}{E_i^2} \frac{I_H}{E_j - E_i} f(ji) g \pi a_0^2 \tag{38}$$

where $f(ij)$ is the oscillator strength, E_i and E_j are the energies of the two states, I_H is the ionization energy of the hydrogen atom, and a_0 is the Bohr radius. The Gaunt factor g may be determined by extensive calculations, [17]

$$g(E_i, E_j) = \frac{8\pi}{\sqrt{3}} \sum_{l_i m_i l_j m_j \mu} |(E_i l_i m_i | r^{-2} Y_{1\mu} | E_j l_j m_j)|^2 \tag{39}$$

or by using approximations based on semi-empirical fitting,

$$g \propto \frac{\sigma_{ij}}{f(ij)} \tag{40}$$

depending on theoretical data of the cross section.

4.4.1 Shevelko's approximation

Based on the semiemperical Lotz formula for ionization of positive ions by electrons,

$$\sigma = 2.76 q (Ry/I)^2 \left(\frac{\ln(u+1)}{u+1} \right)^2 [\pi a_0^2] \tag{41}$$

where I is the binding energy of the shell nl^q, q is the number of equivalent electrons and $u = E/I - 1$ is the scaled incident electron energy. The Maxwellian ionization rate coefficient corresponding to the cross section is,

$$< v\sigma >= 6q\sqrt{\beta} (Ry/I)^2 \exp\{-\beta\} f(\beta) \times 10^{-8} \text{ cm}^3\text{s}^{-1} \tag{42}$$

where the function $f(\beta)$, with $\beta = I/T$ the ratio of the binding energy over the electron temperature, is given by,

$$f(\beta) = e^\beta |Ei(-\beta)| \tag{43}$$

where $Ei(x)$ is the integral exponent. $f(\beta)$ is approximated by,

$$f(\beta) = \ln\left(1 + \frac{0.562 + 1.4\beta}{\beta + 1.4\beta^2}\right) \tag{44}$$

to fit within 3% of the data [18]. This function is used by Hansen et al. [1],

$$\bar{g} = 0.15 + 0.28\ln\left(1 + \frac{0.562 + 1.4\beta}{\beta + 1.4\beta^2}\right) \tag{45}$$

and Sheil et al. [7],

$$\bar{g} = 0.6 + 0.28\ln\left(1 + \frac{0.562 + 1.4\beta}{\beta + 1.4\beta^2}\right) \tag{46}$$

to describe the collisional de-excitation rate.

4.4.2 Mewe's approximation

In Mewe's paper [3], the cross section for an induced radiative process is given by,

$$Q_{ij} = 4\pi a_0^2 \left(\frac{2\pi}{\sqrt{3}}\right)\left(\frac{E_H}{E_{ij}}\right)^2 f(ij) g U^{-1} \tag{47}$$

where E_H is the ionization energy of the hydrogen atom, E_{ij} is the transition energy, oscillator strength $f(ij)$ and $U = E/E_{ij}$ is the ratio of the energy of the impinging electron to the transition energy. Here, the effective gaunt factor g is some average constant value between 0.2 and 0.3. To cover a wider range of transitions, the following description for the effective gaunt factor is proposed,

$$g(U) = A + BU^{-1} + CU^{-2} + D\ln(U) \tag{48}$$

and when integrating the product of the cross section and the electron velocity over a Maxwellian distribution, the excitation rate coefficient is calculated,

$$S_{ij} = 1.70 \times 10^{-3} \cdot T_e^{-1/2} E_{ij}^{-1} f_{ij} \bar{g}(y) 10^{-5040 E_{ij}/T_e} \ \mathrm{cm^3 s^{-1}} \tag{49}$$

with electron temperature T_e and integrated Gaunt factor $\bar{g}$ is given by,

$$\begin{aligned} \bar{g} &= y \exp\{y\} \int_1^\infty e^{-yU} U dU \\ &= A + (By - Cy^2 + D) e^y E_1(y) + Cy \end{aligned} \tag{50}$$

where $y = E_{21}/T_\mathrm{e}$ is the ratio of the energy difference between the two levels and the electron temperature, and $E_1(y)$ is the exponential integral function defined as $E_1(y) = \int_y^\infty \frac{e^{-t}}{t} dt$.

On the surface, A, B and C seems to be free parameters that can be adjusted to fit theoretical and experimental data, but Davis [19] states that for the following description of the effective gaunt factor,

$$\bar{g} = A + BU^{-1} + D\ln(U) \tag{51}$$

the A defines the threshold value, B is connected to the short range part of the potential and D describes the optical properties of the target ion.

Using an approximation for the exponential integral function,

$$e^y E_1(y) \approx \ln\left(\frac{y+1}{y}\right) - \frac{0.4}{(y+1)^2} \qquad \text{for } 0 < y < 10 \tag{52}$$

which is within 3.5 % of the data and using $A = 0.15$ for $\Delta n = 0$ and $A = 0.6$ for $\Delta n \neq 0$, $B = C = 0$ and $D = 0.28$, the integrated Gaunt factors are,

$$\bar{g} = 0.6 + 0.28 \left[\ln\left(\frac{y+1}{y}\right) - \frac{0.4}{(y+1)^2} \right] \qquad \text{for } \Delta n = 0 \tag{53}$$

$$\bar{g} = 0.15 + 0.28 \left[\ln\left(\frac{y+1}{y}\right) - \frac{0.4}{(y+1)^2} \right] \qquad \text{for } \Delta n \neq 0 \tag{54}$$

both of which depend on the ratio of the excitation energy between the two levels to the electron temperature, as well as on the type of transition, characterized by the change in principal quantum number Δn between the levels.

4.4.3 Younger-Wiese's Gaunt factor

In the work of Younger and Wiese [4], the effective Gaunt factor $\bar{g}$ is obtained empirically using theoretical data for the excitation cross section for the excitation of an ion from state i to state j for $\Delta n = 0$ transitions,

$$\bar{g} = \frac{\sqrt{3}}{8\pi} \frac{E_i \Delta E_{ij}}{f_{ij}} Q_{ij} \tag{55}$$

where E_i and E_{ij} are the incident and transition energy (in units of Rydbergs), and f_{ij} is the optical oscillator strength. Based on the data of effective Gaunt factors for electron impact excitation of different $\Delta n = 0$ transitions in alkali-like ions, the following fit is proposed,

$$\bar{g} = \left(1 - \frac{1}{Z_e}\right) \left(0.7 + \frac{1}{n}\right) \left(0.6 + 0.25 \ln\left(\frac{E_i}{\Delta E_{ij}}\right)\right) \tag{56}$$

where n is the principal quantum number and Z_e is the effective nuclear charge of the ion,

$$Z_e = Z - \sigma \tag{57}$$

which is the difference of the atomic number Z - given by the number of protons in the nucleus - and shielding constant σ, which depends on the electron configuration. Looking at two relevant cases, Sn^{11+} and Sn^{14+} ions, the screening constant can be found using Slater's rules by first writing out the electron configuration,

$$\begin{aligned} Sn^{11+} &: 1s^2 2s^2 2p^6 3s^2 3p^6 4s^2 3d^{10} 4p^6 4d^3 \\ Sn^{14+} &: 1s^2 2s^2 2p^6 3s^2 3p^6 4s^2 3d^{10} 4p^6 \end{aligned} \tag{58}$$

then rearranging the terms based on the principal quantum number,

$$\begin{aligned} Sn^{11+} &: 1s^2 \quad 2s^2 2p^6 \quad 3s^2 3p^6 3d^{10} \quad 4s^2 4p^6 4d^3 \\ Sn^{14+} &: 1s^2 \quad 2s^2 2p^6 \quad 3s^2 3p^6 3d^{10} \quad 4s^2 4p^6 \end{aligned} \tag{59}$$

and depending on the angular momentum quantum number l of the electron for which the screening constant is calculated, the following rules apply [20]:

- For a d or f electron, like in the case of Sn^{11+}, add 0.35 for each electron in the same group or having the same n quantum number and add 1.00 for every electron in a lower group.

$$\sigma_{Sn^{11+}} = 0.35 \times (11 - 1) + 1.00 \times (2 + 8 + 18) = 31.5 \Rightarrow Z_e = 50 - 31.5 = 18.5 \tag{60}$$

- For a s or p electron, like in the case of Sn^{14+}, add 0.35 for each electron in the same group, 0.85 for each electron in one shell lower and 1.00 for every electron in a shell below that.

$$\sigma_{Sn^{14+}} = 0.35\times(8-1)+0.85\times 18+1.00\times(2+8) = 27.75 \Rightarrow Z_e = 50-27.75 = 22.25 \quad (61)$$

5 Results

5.1 Impact of key parameters on population distribution

5.1.1 Electron density

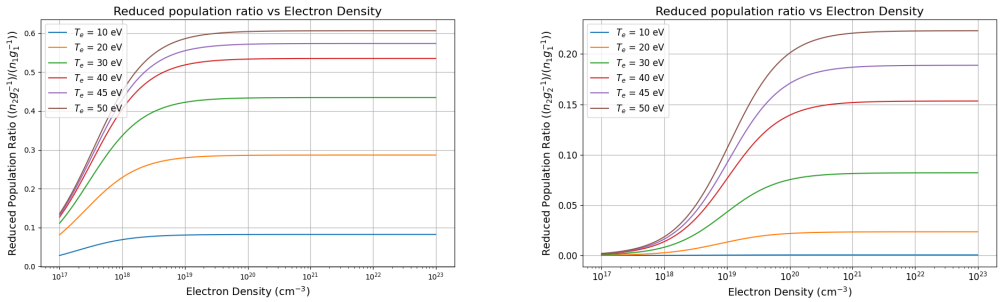

(a) $E_{21} = 25$ eV (b) $E_{21} = 75$ eV

Figure 2: Dependency of the reduced population ratio on the electron density n_e for different T_e at two different values for E_{21}.

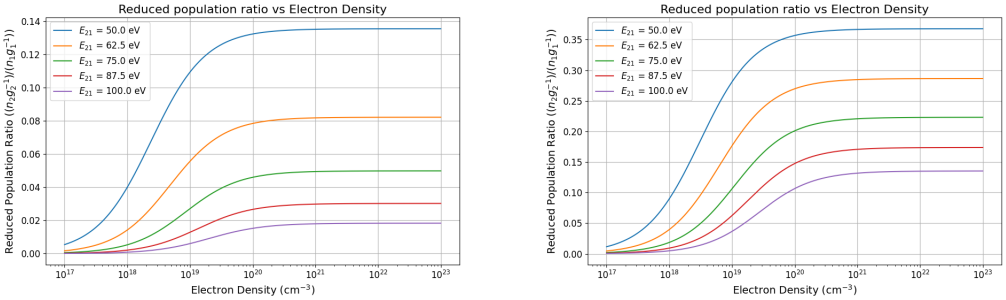

(a) $T_e = 25$ eV (b) $T_e = 50$ eV

Figure 3: Dependency of the reduced population ratio on the electron density n_e for different E_{21} at two different values for T_e.

In figs. 2 and 3, the reduced population ratio is plotted as a function of the electron density n_e. All plots converge to a constant reduced population ratio that is dependent on the electron temperature and excitation energy. In figs. 2a and 2b, we see that the reduced population ratio increases with the electron temperature. In figs. 3a and 3b, we see that the reduced population ratio decreases with the excitation energy. For all plots, we see that the ratio increases exponentially with n_e, and then converges to $\exp\{-E_{21}/T_e\}$ (see Eqs. 14 and 15).

5.1.2 Excitation energy

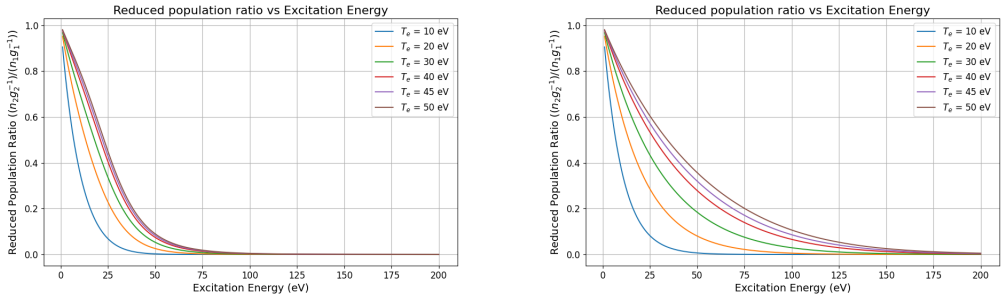

(a) $n_e = 10^{18}$ cm^{-3} (b) $n_e = 10^{20}$ cm^{-3}

Figure 4: Dependency of the reduced population ratio on the excitation energy E_{21} for different T_e at two different values for n_e.

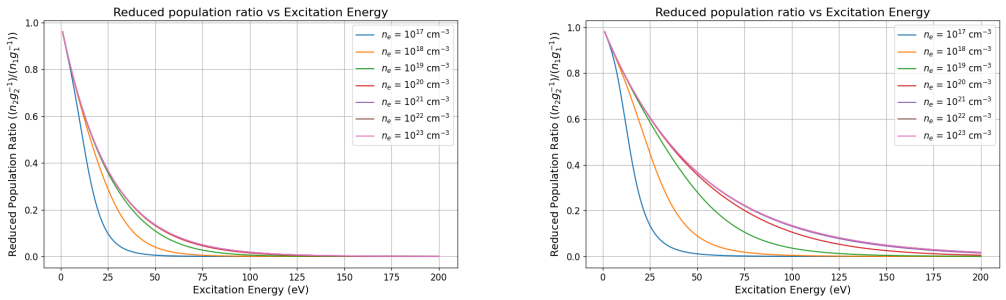

(a) $T_e = 25$ eV (b) $T_e = 50$ eV

Figure 5: Dependency of the reduced population ratio on the excitation energy E_{21} for at different n_e at two different values for T_e.

Figs. 4 and 5 show the plots of the reduced population ratio as a function of the excitation energy. We see that in all the plots that the reduced population ratio approaches one as the excitation energy goes to zero and approaches zero as the excitation energy becomes very large. Figs. 4a and 4b show that the reduced population ratio increases with electron temperature T_e and figs. 5a and 5b show that it also increases with electron density n_e. This is what is expected based on Eqs. 18 and 19. Another interesting aspect is that as the electron temperature or density increases, the change in the reduced population ratio becomes weaker.

5.1.3 Electron temperature

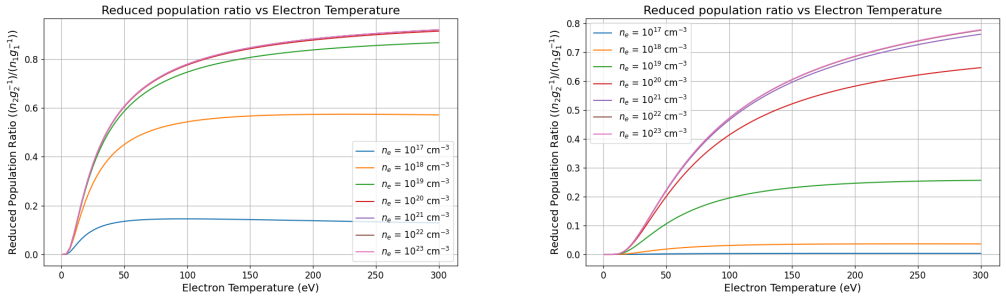

(a) $E_{21} = 25$ eV (b) $E_{21} = 75$ eV

Figure 6: Dependency of the reduced population ratio on the electron temperature T_e for different n_e at two different values of E_{21}.

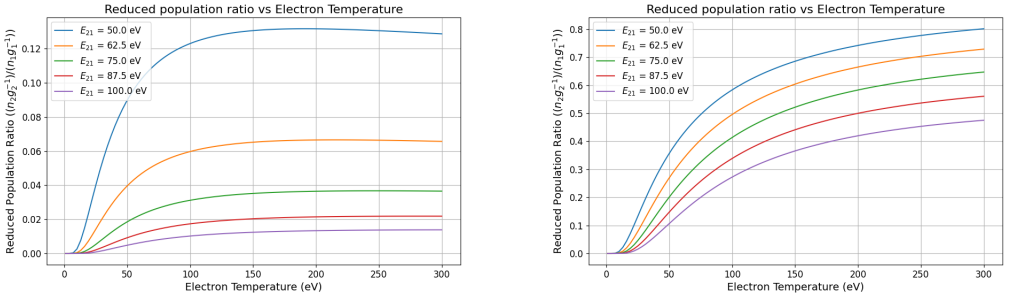

(a) $n_e = 10^{18}$ cm^{-3} (b) $n_e = 10^{20}$ cm^{-3}

Figure 7: Dependency of the reduced population ratio on the electron temperature T_e for at different E_{21} for two different values of n_e.

Figs. 6 and 7 display the reduced population ratio with respect to the electron temperature. We see that the reduced population ratio first increases with T_e, then reaches a maximum value, and finally decreases. This behaviour corresponds with Eqs. 22, 28 and 23, which describe the behaviour of the reduced population ratio with respect to the electron temperature. Figs. 6a and 6b show that the reduced population ratio increases with the electron density n_e and figs. 7a and 7b show that it decreases with excitation energy E_{21}. Furthermore, as electron density increases, the change in the reduced population ratio becomes weaker as is shown in fig. 6.

5.2 Effective temperature in hot plasmas

5.2.1 Electron density

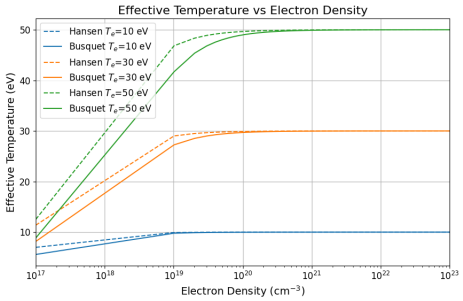

(a) $E_{21} = 25$ eV

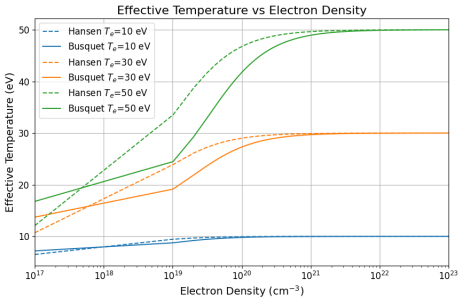

(b) $E_{21} = 75$ eV

Figure 8: Effective temperatures varying with n_e for different T_e at two different values for E_{21}.

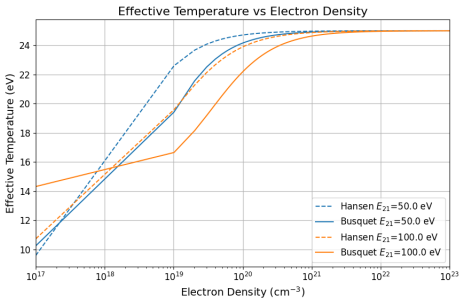

(a) $T_e = 25$ eV

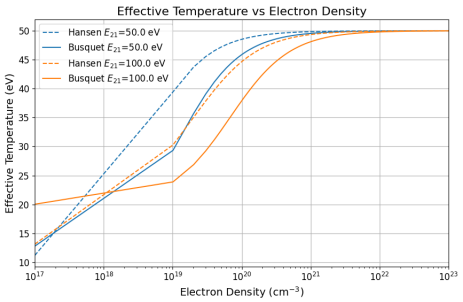

(b) $T_e = 50$ eV

Figure 9: Effective temperatures varying with n_e for different E_{21} at two different values for T_e.

Figs. 8 and 9 show the effective temperature as a function of the electron density. The plot consists of two parts, a linearly increasing domain until 10^{19} cm^{-3}, after which the effective temperature converges to the electron temperature. When we look at figs. 8a and 8b, we see that the effective temperature increases with the electron temperature. From figs. 9a and 9b, we see that the effective temperature decreases with the electron density. While looking at the low electron densities limit, it was found that for electron densities approaching zero, Busquet's model does not predict an effective temperature of zero.

5.2.2 Excitation energy

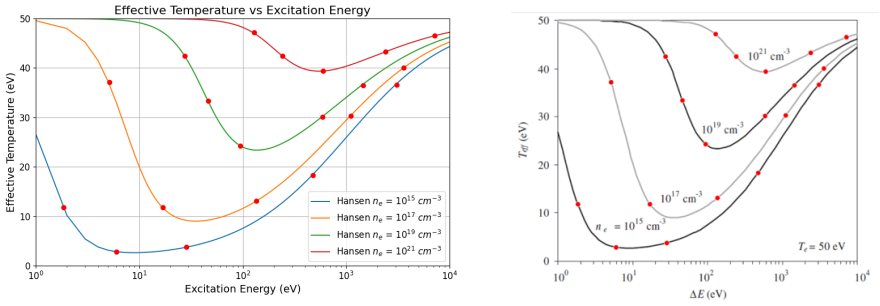

(a) Effective temperature (b) Figure 6 left from Hansen et al.

Figure 10: Effective temperatures varying with n_e for different n_e. Recreating plot from Hansen et al. [1]

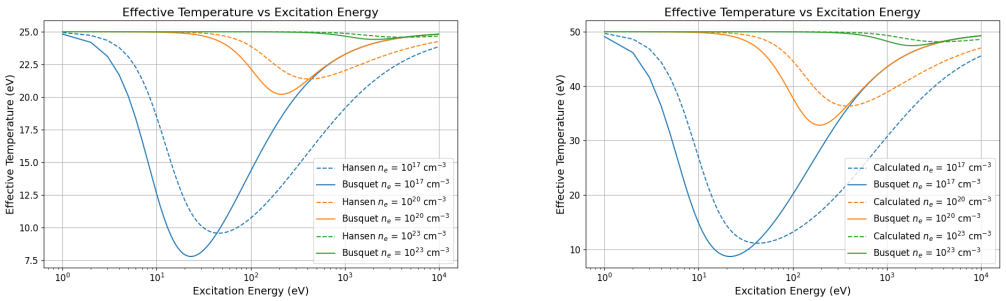

(a) $T_e = 25$ eV (b) $T_e = 50$ eV

Figure 11: Effective temperatures varying with E_{21} for different n_e at two different values for T_e.

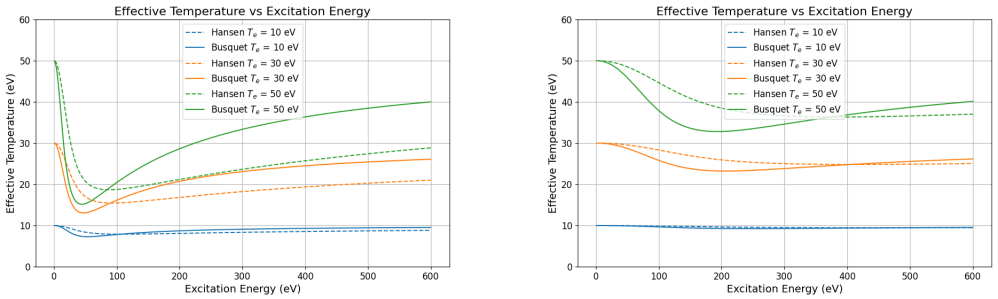

(a) $n_e = 10^{18}$ cm^{-3} (b) $n_e = 10^{20}$ cm^{-3}

Figure 12: Effective temperatures varying with E_{21} for different T_e at two different values for n_e.

To compare the model with literature, the effective temperature as a function of the excitation

energy E_{21} is plotted and compared with the results from Hansen et al. [1]. These results are in agreement (see fig. 10).

Figs. 11 and 12 show that the curves converge towards the electron temperature as the excitation energy goes to zero or infinity. Looking at 11a and 11b, we see that the effective temperature increases with the electron density. From figs. 12a and 12b, we see that the effective temperature increases with the electron temperature.

When comparing the two models, it can be seen that the minimum effective temperature of the Busquet model is lower and at a lower excitation energy than Hansen's model. Another remarkable observation is that Hansen's model predicts a higher effective temperature until the minimum is reached, after which the Busquet model predicts a higher effective temperature.

5.2.3 Electron temperature

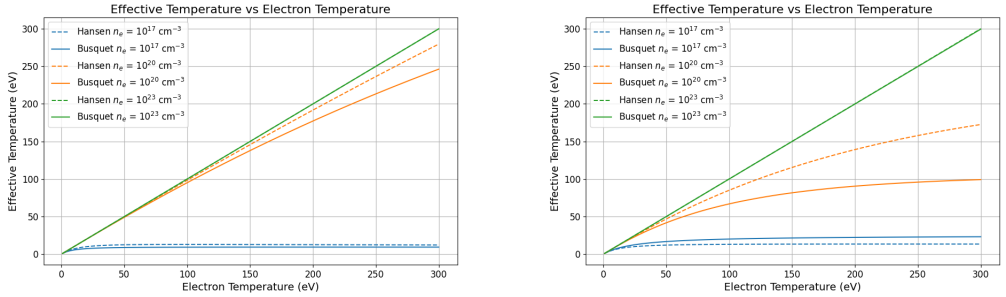

(a) $E_{21} = 25$ eV (b) $E_{21} = 75$ eV

Figure 13: Effective temperatures varying with T_e for different n_e at two different values for E_{21}.

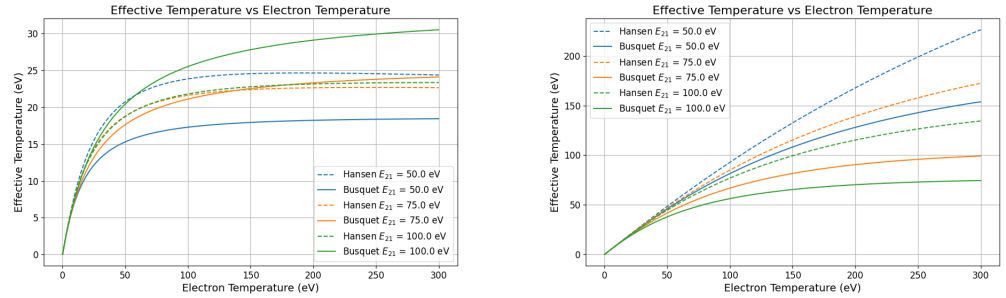

(a) $n_e = 10^{18}$ cm^{-3} (b) $n_e = 10^{20}$ cm^{-3}

Figure 14: Effective temperatures varying with T_e for different E_{21} at two different values for n_e.

Figs. 13 and 14 describe the behaviour of the effective temperature as a function of the electron temperature. The effective temperature increases linearly at low electron temperatures. This is due to the effective temperature being approximately equal to the electron temperature at lower electron temperatures. Figs. 13a and 13b show that this linearity falls off more rapidly as the electron density decreases. Figs. 14a and 14b show a similar trend for increasing excitation energies.

5.3 Gaunt factor

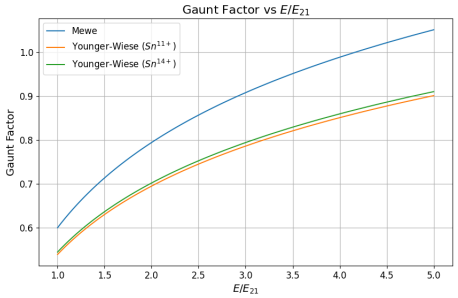

(a) Gaunt factor vs. incident energy over transition energy. Here the Gaunt factor is plotted for Sn^{11+} and Sn^{14+}, where for both $n = 4$.

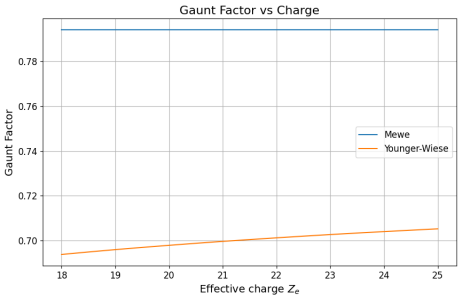

(b) Gaunt factor vs. effective charge. Here the Gaunt factor is plotted a range of effective charges, with principle quantum number $n = 4$.

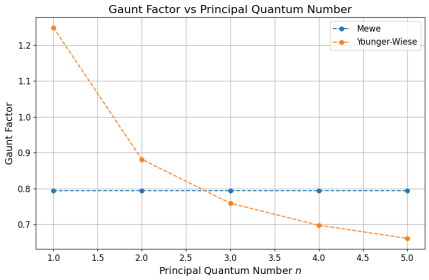

Figure 16: Gaunt factor vs. principal quantum number n. Here the Gaunt factor is plotted with an effective charge of 20 and $E/E_{21} = 2$.

Fig. 15a shows the Gaunt factor as function of the ratio of the incident energy over the transition energy. When looking at the plot and comparing both models over the same domain, we see that Mewe's Gaunt factor is consistently higher than that of Younger and Wiese.

Fig. 15b shows the Gaunt factor as function of the effective charge. Again, we see that Mewe's Gaunt factor is consistently higher than that of Younger and Wiese. Since Mewe's model does not depend on the charge, Mewe's Gaunt factor remains constant across different effective charges.

Finally, Fig. 16 shows the Gaunt factor as function of the principle quantum number n. Mewe's Gaunt factor is constant across different values of n, while Younger and Wiese's Gaunt factor varies with n. For lower values of n, Younger and Wiese's Gaunt factor is higher than Mewe's, while for higher values of n, Mewe's Gaunt factor becomes higher.

6 Three-Level Model

Until this point, the system has been described with two levels and three kinds of processes. For the sake of simplicity, the kinds of processes will not change. In this section, the model is extended to include a third level, allowing for a more comprehensive description of the system's dynamics. There are two possible ways to extend the model: interacting and non-interacting excited states. To get an expression for the population dynamics, the same approach is used as in section 4.1.

6.1 Non-Interacting Excited States

In the non-interacting excited state model, both excited states are independent of each other. This means that the collisional and radiative processes occur between the ground state and the excited states, which is represented in the following diagram.

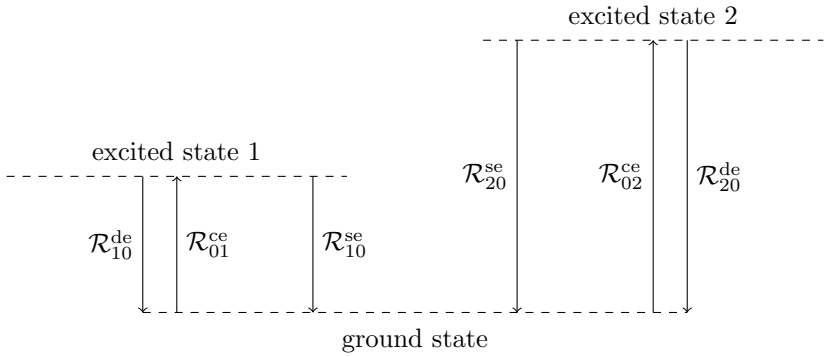

Figure 17: Three-level model with non-interacting excited states. The ground state, excited state 1 and excited state 2 have a population density of n_0, n_1 and n_2, respectively, and corresponding energies E_0, E_1 and E_2. The energy of excited state 2 is higher than that of excited state 1, which is higher than that of the ground state, $E_2 > E_1 > E_0$.

Using the system of collisional-radiative rate equations,

$$\frac{\mathrm{d}n_i}{\mathrm{d}t} = \sum_p \sum_{k \neq i} n_k \mathcal{R}^p_{ki} - n_i \sum_p \sum_{k \neq i} \mathcal{R}^p_{ik} \tag{62}$$

the rate equation for each level can be derived,

$$\begin{aligned} \frac{dn_0}{\mathrm{d}t} &= n_1\mathcal{R}^{\mathrm{de}}_{10} - n_0\mathcal{R}^{\mathrm{ce}}_{01} + n_1\mathcal{R}^{\mathrm{se}}_{10} + n_2\mathcal{R}^{\mathrm{se}}_{20} - n_0\mathcal{R}^{\mathrm{ce}}_{02} + n_2\mathcal{R}^{\mathrm{de}}_{20} \\ &= n_1(\mathcal{R}^{\mathrm{de}}_{10} + \mathcal{R}^{\mathrm{se}}_{10}) + n_2(\mathcal{R}^{\mathrm{de}}_{20} + \mathcal{R}^{\mathrm{se}}_{20}) - n_0(\mathcal{R}^{\mathrm{ce}}_{01} + \mathcal{R}^{\mathrm{ce}}_{02}) \end{aligned} \tag{63}$$

$$\frac{dn_1}{\mathrm{d}t} = -n_1\mathcal{R}^{\mathrm{de}}_{10} + n_0\mathcal{R}^{\mathrm{ce}}_{01} - n_1\mathcal{R}^{\mathrm{se}}_{10} = n_0\mathcal{R}^{\mathrm{ce}}_{01} - n_1(\mathcal{R}^{\mathrm{de}}_{10} + \mathcal{R}^{\mathrm{se}}_{10}) \tag{64}$$

$$\frac{dn_2}{\mathrm{d}t} = -n_2\mathcal{R}^{\mathrm{se}}_{02} + n_0\mathcal{R}^{\mathrm{ce}}_{02} - n_2\mathcal{R}^{\mathrm{de}}_{20} = n_0\mathcal{R}^{\mathrm{ce}}_{02} - n_2(\mathcal{R}^{\mathrm{de}}_{20} + \mathcal{R}^{\mathrm{se}}_{20}) \tag{65}$$

and using the concept of steady state,

$$\frac{dn_0}{\mathrm{d}t} = \frac{dn_1}{\mathrm{d}t} = \frac{dn_2}{\mathrm{d}t} = 0 \tag{66}$$

the principle of detailed balance,

$$n_1\mathcal{R}_{10}^{\mathrm{de}} = n_0\mathcal{R}_{01}^{\mathrm{ce}} \qquad \& \qquad n_2\mathcal{R}_{20}^{\mathrm{de}} = n_0\mathcal{R}_{02}^{\mathrm{ce}} \tag{67}$$

the following relationships can be derived:

- $\dfrac{dn_2}{\mathrm{d}t} = 0$

$$\begin{aligned} n_0\mathcal{R}_{02}^{\mathrm{ce}} &= n_2\left(\mathcal{R}_{20}^{\mathrm{de}} + \mathcal{R}_{20}^{\mathrm{se}}\right) \\ \frac{n_0}{n_2} &= \frac{\mathcal{R}_{20}^{\mathrm{de}} + \mathcal{R}_{20}^{\mathrm{se}}}{\mathcal{R}_{02}^{\mathrm{ce}}} \\ &= \frac{n_0}{n_2}\left(1 + \frac{\mathcal{R}_{20}^{\mathrm{se}}}{\mathcal{R}_{20}^{\mathrm{de}}}\right) \end{aligned} \tag{68}$$

- $\dfrac{dn_1}{\mathrm{d}t} = 0$

$$\begin{aligned} n_0\mathcal{R}_{01}^{\mathrm{ce}} &= n_1\left(\mathcal{R}_{10}^{\mathrm{de}} + \mathcal{R}_{10}^{\mathrm{se}}\right) \\ \frac{n_0}{n_1} &= \frac{\mathcal{R}_{10}^{\mathrm{de}} + \mathcal{R}_{10}^{\mathrm{se}}}{\mathcal{R}_{01}^{\mathrm{ce}}} \\ &= \frac{n_0}{n_1}\left(1 + \frac{\mathcal{R}_{10}^{\mathrm{se}}}{\mathcal{R}_{10}^{\mathrm{de}}}\right) \end{aligned} \tag{69}$$

To get to the final expression, use Boltzmann statistics,

$$\frac{n_0}{n_1} = \frac{g_0}{g_1}\exp\left\{-\frac{E_{01}}{T_e}\right\} \qquad \& \qquad \frac{n_0}{n_2} = \frac{g_0}{g_2}\exp\left\{-\frac{E_{02}}{T_e}\right\} \tag{70}$$

where $E_{ij} \equiv E_i - E_j$. The expressions for the rates of the processes from level i to level j, where $i > j$ (since these processes are always from a higher to a lower level),

$$\mathcal{R}_{ij}^{\mathrm{se}} = \mathcal{C}^{\mathrm{se}} f_{ij}(E_i - E_j)^2 \qquad \text{with} \qquad \mathcal{C}^{\mathrm{se}} = 4.3 \times 10^7 \text{ eV}^{-2} \text{ s}^{-1} \tag{71}$$

$$\mathcal{R}_{ij}^{\mathrm{de}} = \mathcal{C}^{\mathrm{de}} \frac{n_e f_{ij} \bar{g}_{ij}}{(E_i - E_j)\sqrt{T_e}} \qquad \text{with} \qquad \mathcal{C}^{\mathrm{de}} = 1.6 \times 10^{-5} \text{ eV}^{3/2} \text{ cm}^3 \text{ s}^{-1} \tag{72}$$

to obtain the population density ratios,

$$\frac{n_0}{n_1} = \frac{g_0}{g_1}\exp\left\{-\frac{E_{01}}{T_e}\right\}\left(1 + \frac{\mathcal{C}E_{10}^3\sqrt{T_e}}{n_e\bar{g}_{10}}\right) \Longleftrightarrow \frac{n_1}{n_0} = \frac{g_1}{g_0}\exp\left\{-\frac{E_{10}}{T_e}\right\}\left(1 + \frac{\mathcal{C}E_{10}^3\sqrt{T_e}}{n_e\bar{g}_{10}}\right)^{-1} \tag{73}$$

$$\frac{n_0}{n_2} = \frac{g_0}{g_2}\exp\left\{-\frac{E_{02}}{T_e}\right\}\left(1 + \frac{\mathcal{C}E_{20}^3\sqrt{T_e}}{n_e\bar{g}_{20}}\right) \Longleftrightarrow \frac{n_2}{n_0} = \frac{g_2}{g_0}\exp\left\{-\frac{E_{20}}{T_e}\right\}\left(1 + \frac{\mathcal{C}E_{20}^3\sqrt{T_e}}{n_e\bar{g}_{20}}\right)^{-1} \tag{74}$$

where $\mathcal{C} = \mathcal{C}^{\mathrm{se}}/\mathcal{C}^{\mathrm{de}} = 2.69 \times 10^{12}$ eV$^{-7/2}$ cm^{-3}. Notice that the result is that this system seems to be described by two independent two-level systems, one for each excited state.

6.2 Interacting Excited States

In the interacting excited state model, the excited states can interact with the ground state and with each other. This can be represented in the following diagram.

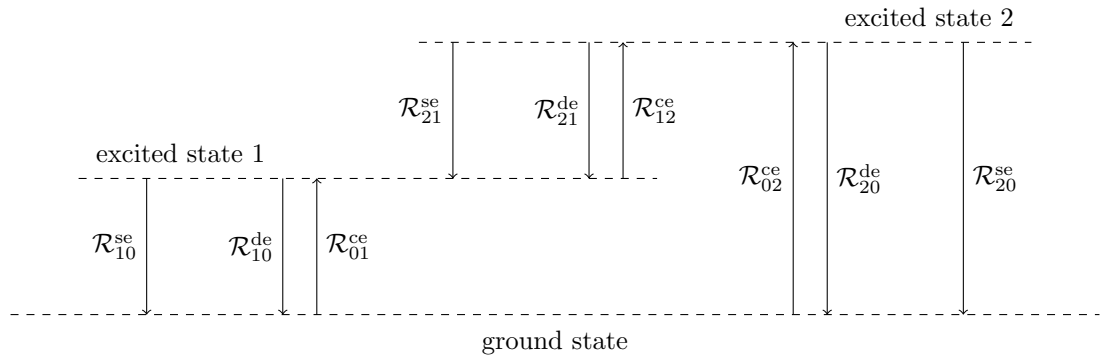

Figure 18: Three-level model with interacting excited states. The ground state, excited state 1 and excited state 2 have a population density of n_0, n_1 and n_2, respectively, and corresponding energies E_0, E_1 and E_2. Needless to say, energy of excited state 2 is higher than that of excited state 1, which is higher than that of the ground state, $E_2 > E_1 > E_0$.

Following the same approach as in the previous subsection, the rate equations for this case are:

$$\begin{aligned}\frac{dn_0}{\mathrm{d}t} &= n_1\mathcal{R}_{10}^{\text{se}} + n_1\mathcal{R}_{10}^{\text{de}} - n_0\mathcal{R}_{01}^{\text{ce}} - n_0\mathcal{R}_{02}^{\text{ce}} + n_2\mathcal{R}_{20}^{\text{de}} + n_2\mathcal{R}_{20}^{\text{se}} \\ &= n_1(\mathcal{R}_{10}^{\text{de}} + \mathcal{R}_{10}^{\text{se}}) + n_2(\mathcal{R}_{20}^{\text{de}} + \mathcal{R}_{20}^{\text{se}}) - n_0(\mathcal{R}_{01}^{\text{ce}} + \mathcal{R}_{02}^{\text{ce}})\end{aligned} \tag{75}$$

$$\begin{aligned}\frac{dn_1}{\mathrm{d}t} &= -n_1\mathcal{R}_{10}^{\text{se}} - n_1\mathcal{R}_{10}^{\text{de}} + n_0\mathcal{R}_{01}^{\text{ce}} + n_2\mathcal{R}_{21}^{\text{se}} + n_2\mathcal{R}_{21}^{\text{de}} - n_1\mathcal{R}_{12}^{\text{ce}} \\ &= n_0\mathcal{R}_{01}^{\text{ce}} + n_2(\mathcal{R}_{21}^{\text{de}} + \mathcal{R}_{21}^{\text{se}}) - n_1(\mathcal{R}_{10}^{\text{de}} + \mathcal{R}_{10}^{\text{se}} + \mathcal{R}_{12}^{\text{ce}})\end{aligned} \tag{76}$$

$$\begin{aligned}\frac{dn_2}{\mathrm{d}t} &= -n_2\mathcal{R}_{21}^{\text{se}} - n_2\mathcal{R}_{21}^{\text{de}} + n_1\mathcal{R}_{12}^{\text{ce}} + n_0\mathcal{R}_{02}^{\text{ce}} - n_2\mathcal{R}_{20}^{\text{de}} + n_2\mathcal{R}_{20}^{\text{se}} \\ &= n_0\mathcal{R}_{02}^{\text{ce}} + n_1\mathcal{R}_{12}^{\text{ce}} - n_2(\mathcal{R}_{20}^{\text{de}} + \mathcal{R}_{20}^{\text{se}} + \mathcal{R}_{21}^{\text{de}} + \mathcal{R}_{21}^{\text{se}})\end{aligned} \tag{77}$$

Using the concept of steady state,

$$\frac{dn_0}{\mathrm{d}t} = \frac{dn_1}{\mathrm{d}t} = \frac{dn_2}{\mathrm{d}t} = 0 \tag{78}$$

the principle of detailed balance,

$$n_1\mathcal{R}_{10}^{\text{de}} = n_0\mathcal{R}_{01}^{\text{ce}} \qquad \& \qquad n_2\mathcal{R}_{20}^{\text{de}} = n_0\mathcal{R}_{02}^{\text{ce}} \qquad \& \qquad n_2\mathcal{R}_{21}^{\text{de}} = n_1\mathcal{R}_{12}^{\text{ce}} \tag{79}$$

and Boltzmann statistics,

$$\frac{n_0}{n_1} = \frac{g_0}{g_1}\exp\left\{-\frac{E_{01}}{T_e}\right\} \quad \& \quad \frac{n_0}{n_2} = \frac{g_0}{g_2}\exp\left\{-\frac{E_{02}}{T_e}\right\} \quad \& \quad \frac{n_1}{n_2} = \frac{g_1}{g_2}\exp\left\{-\frac{E_{12}}{T_e}\right\} \tag{80}$$

the following relationships can be derived:

- $\dfrac{dn_2}{\mathrm{d}t} = 0$

$$\begin{aligned} n_0\mathcal{R}_{02}^{\mathrm{ce}} + n_1\mathcal{R}_{12}^{\mathrm{ce}} &= n_2\left(\mathcal{R}_{20}^{\mathrm{de}} + \mathcal{R}_{20}^{\mathrm{se}} + \mathcal{R}_{21}^{\mathrm{de}} + \mathcal{R}_{21}^{\mathrm{se}}\right) \\ \frac{n_0}{n_2} &= \frac{\mathcal{R}_{20}^{\mathrm{de}} + \mathcal{R}_{20}^{\mathrm{se}} + \mathcal{R}_{21}^{\mathrm{de}} + \mathcal{R}_{21}^{\mathrm{se}}}{\mathcal{R}_{02}^{\mathrm{ce}}} - \frac{n_1\mathcal{R}_{12}^{\mathrm{ce}}}{n_2\mathcal{R}_{02}^{\mathrm{ce}}} \\ &= \frac{\mathcal{R}_{20}^{\mathrm{de}} + \mathcal{R}_{20}^{\mathrm{se}} + \mathcal{R}_{21}^{\mathrm{se}}}{\mathcal{R}_{02}^{\mathrm{ce}}} + \frac{\mathcal{R}_{21}^{\mathrm{de}}}{\mathcal{R}_{02}^{\mathrm{ce}}} - \cancelto{0}{\frac{n_2\mathcal{R}_{21}^{\mathrm{de}}}{n_2\mathcal{R}_{02}^{\mathrm{ce}}}} \\ &= \frac{\mathcal{R}_{20}^{\mathrm{de}} + \mathcal{R}_{20}^{\mathrm{se}} + \mathcal{R}_{21}^{\mathrm{se}}}{\frac{n_2}{n_0}\mathcal{R}_{20}^{\mathrm{de}}} = \frac{n_0}{n_2}\left(1 + \frac{\mathcal{R}_{20}^{\mathrm{se}} + \mathcal{R}_{21}^{\mathrm{se}}}{\mathcal{R}_{20}^{\mathrm{de}}}\right) \end{aligned} \tag{81}$$

- $\dfrac{dn_1}{\mathrm{d}t} = 0$

$$\begin{aligned} n_0\mathcal{R}_{01}^{\mathrm{ce}} + n_2(\mathcal{R}_{21}^{\mathrm{de}} + \mathcal{R}_{21}^{\mathrm{se}}) &= n_1\left(\mathcal{R}_{10}^{\mathrm{de}} + \mathcal{R}_{10}^{\mathrm{se}} + \mathcal{R}_{12}^{\mathrm{ce}}\right) \\ \frac{n_2}{n_1} &= \frac{\mathcal{R}_{10}^{\mathrm{de}} + \mathcal{R}_{10}^{\mathrm{se}} + \mathcal{R}_{12}^{\mathrm{ce}}}{\mathcal{R}_{21}^{\mathrm{de}} + \mathcal{R}_{21}^{\mathrm{se}}} - \frac{n_0\mathcal{R}_{01}^{\mathrm{ce}}}{n_1(\mathcal{R}_{21}^{\mathrm{de}} + \mathcal{R}_{21}^{\mathrm{se}})} \\ &= \frac{\mathcal{R}_{10}^{\mathrm{se}} + \mathcal{R}_{12}^{\mathrm{ce}}}{\mathcal{R}_{21}^{\mathrm{de}} + \mathcal{R}_{21}^{\mathrm{se}}} + \frac{\mathcal{R}_{10}^{\mathrm{de}}}{\mathcal{R}_{21}^{\mathrm{de}} + \mathcal{R}_{21}^{\mathrm{se}}} - \cancelto{0}{\frac{n_1\mathcal{R}_{10}^{\mathrm{de}}}{n_1(\mathcal{R}_{21}^{\mathrm{de}} + \mathcal{R}_{21}^{\mathrm{se}})}} \\ &= \frac{\mathcal{R}_{10}^{\mathrm{se}}}{\mathcal{R}_{21}^{\mathrm{de}} + \mathcal{R}_{21}^{\mathrm{se}}} + \frac{\mathcal{R}_{12}^{\mathrm{ce}}}{\mathcal{R}_{21}^{\mathrm{de}} + \mathcal{R}_{21}^{\mathrm{se}}} \\ &= \frac{\mathcal{R}_{10}^{\mathrm{se}}}{\mathcal{R}_{21}^{\mathrm{de}} + \mathcal{R}_{21}^{\mathrm{se}}} + \frac{n_2}{n_1}\frac{\mathcal{R}_{21}^{\mathrm{de}}}{\mathcal{R}_{21}^{\mathrm{de}} + \mathcal{R}_{21}^{\mathrm{se}}} \\ 1 &= \frac{n_1}{n_2}\frac{\mathcal{R}_{10}^{\mathrm{se}}}{\mathcal{R}_{21}^{\mathrm{de}} + \mathcal{R}_{21}^{\mathrm{se}}} + \frac{\mathcal{R}_{21}^{\mathrm{de}}}{\mathcal{R}_{21}^{\mathrm{de}} + \mathcal{R}_{21}^{\mathrm{se}}} \\ \frac{n_1}{n_2} &= \frac{\mathcal{R}_{21}^{\mathrm{de}} + \mathcal{R}_{21}^{\mathrm{se}}}{\mathcal{R}_{10}^{\mathrm{se}}} - \frac{\mathcal{R}_{21}^{\mathrm{de}}}{\mathcal{R}_{10}^{\mathrm{se}}} = \frac{\mathcal{R}_{21}^{\mathrm{se}}}{\mathcal{R}_{10}^{\mathrm{se}}} \end{aligned} \tag{82}$$

Using the expressions for the rates of the processes (Eqs. 71, 72) the population density ratios can be obtained,

$$\begin{aligned} \frac{n_0}{n_2} &= \frac{g_0}{g_2}\exp\left\{-\frac{E_{02}}{T_e}\right\}\left(1 + \frac{\mathcal{C}E_{20}^3\sqrt{T_e}}{n_e\bar{g}_{20}} + \frac{\mathcal{C}f_{21}E_{21}^3\sqrt{T_e}}{f_{20}n_e\bar{g}_{21}}\right) \\ &\iff \frac{n_2}{n_0} = \frac{g_2}{g_0}\exp\left\{-\frac{E_{20}}{T_e}\right\}\left(1 + \frac{\mathcal{C}E_{20}^3\sqrt{T_e}}{n_e\bar{g}_{20}} + \frac{\mathcal{C}f_{21}E_{21}^3\sqrt{T_e}}{f_{20}n_e\bar{g}_{21}}\right)^{-1} \end{aligned} \tag{83}$$

$$\frac{n_1}{n_2} = \frac{f_{21}E_{21}^2}{f_{10}E_{10}^2} \iff \frac{n_2}{n_1} = \frac{f_{10}E_{10}^2}{f_{21}E_{21}^2} \tag{84}$$

$$\begin{aligned} \frac{n_0}{n_1} &= \frac{n_2}{n_1}\frac{n_0}{n_2} = \frac{f_{10}E_{10}^2}{f_{21}E_{21}^2}\frac{g_0}{g_2}\exp\left\{-\frac{E_{02}}{T_e}\right\}\left(1 + \frac{\mathcal{C}E_{20}^3\sqrt{T_e}}{n_e\bar{g}_{20}} + \frac{\mathcal{C}f_{21}E_{21}^3\sqrt{T_e}}{f_{20}n_e\bar{g}_{21}}\right) \\ &\iff \frac{n_1}{n_0} = \frac{n_1}{n_2}\frac{n_2}{n_0} = \frac{f_{21}E_{21}^2}{f_{10}E_{10}^2}\frac{g_2}{g_0}\exp\left\{-\frac{E_{20}}{T_e}\right\}\left(1 + \frac{\mathcal{C}E_{20}^3\sqrt{T_e}}{n_e\bar{g}_{20}} + \frac{\mathcal{C}f_{21}E_{21}^3\sqrt{T_e}}{f_{20}n_e\bar{g}_{21}}\right)^{-1} \end{aligned} \tag{85}$$

where different $\bar{g}$ factors are used since the difference in energy between the levels is different.

7 Conclusion

The goal of the thesis was to study the two-level model. This was done by first deriving the equation for the two-level model and then looking at how the population behaves when changing the excitation energy, the plasma temperature (specifically the electron temperature), and the electron density n_e. From the theory and results, it is clear that the impact of these parameters on the population dynamics is difficult to describe, particularly because the excitation energy and electron temperature interact in a complex way. Nevertheless, the equation does behave intuitively when considering the limiting cases of the parameters, which is also reflected in the plots.

After that, we compared two different approaches to calculate the effective temperature, the one derived from the two-level model, also referred to as the calculated effective temperature, and Busquet approach. When comparing both approaches, we see that in the high-electron-density, high-temperature and high-excitation-energy limit, the results of the calculated effective temperature show a good agreement with Busquet, while at lower values, there is a noticeable deviation between the two approaches.

Subsequently, we looked at the Gaunt factor, which is a factor that influences the radiation rates. There we found that there are multiple formulae that describe this factor. This is due to the approximations made in the different models used to derive the Gaunt factor, leading to variations in the predicted values. Two notable approaches are the one by Mewe and the other by Younger-Wiese. When comparing both equations, we see that both depend on the ratio of the incident energy over the transition energy, but the Younger-Wiese equation also depends on the effective charge and the principle quantum number. When plotting the results, we find that Mewe's Gaunt factor is consistently higher than the Younger-Wiese Gaunt factor when considering the energy ratio. Moreover, varying the effective charge shows that Mewe's Gaunt factor remains constant, and within the relevant ranges of these parameters, it is always greater than the Younger-Wiese Gaunt factor.

Finally, we tried to extend the two level model by adding a third level. This creates two possible models, one where the excited levels interact with each other and one where they do not. For the one where there is no interaction, we found that the model can be described by two two-level models, as intuitively expected and shown based on the equations. The interacting model, however, is more complex and requires a bit of algebraic manipulation to fully describe the population dynamics. Both three level models can be described using a system of two independent equations describing the population ratios between the levels.

For future work, it would be interesting to explore the effects of additional atomic processes on the three-level model. This would greatly impact the equations describing the population dynamics and could lead to a more accurate representation of the plasma behavior. In the same manner, one could also try to see how the population dynamics are affected when taking into account photoabsorption processes driven by an external radiation field. In reality, each plasma region is influenced by a radiation field generated by neighboring regions, which can lead to complex interactions and dependencies.

Additionally, the three level model can be applied on specific atomic transitions, allowing for a more realistic description of the population dynamics in these systems. To give an example, for electric dipole transitions (E1), the parity of the initial and final states cannot be the same, which imposes additional constraints on the ratio of radiative rates.

Finally, the three-level model can be extended to include additional levels, allowing for a more detailed exploration of the population dynamics in complex atomic systems. In that case, it is the goal to derive a general formula for the population ratios by recognizing the patterns and dependencies that emerge from the interactions between the different levels.

References

[1] S. Hansen, K. Fournier, C. Bauche-Arnoult, J. Bauche, and O. Peyrusse, Journal of Quantitative Spectroscopy and Radiative Transfer **99**, 272 (2006).

[2] M. Busquet, Journal of Quantitative Spectroscopy and Radiative Transfer **99**, 131 (2006), radiative Properties of Hot Dense Matter.

[3] R. Mewe, Astronomy and Astrophysics **20**, 215 (1972).

[4] S. Younger and W. Wiese, Journal of Quantitative Spectroscopy and Radiative Transfer **22**, 161 (1979).

[5] R. J. Goldston and P. H. Rutherford, *Introduction to Plasma Physics* (CRC Press, London, 1995).

[6] ASML, "Light & lasers - lithography principles," `https://www.asml.com/en/technology/lithography-principles/light-and-lasers`, accessed: 2025-08-21.

[7] J. Sheil, Y. V. Ralchenko, A. Neukirch, and J. Colgan, "Effective temperatures in hot plasmas: the case of open-n-shell tin ions," (2025), unpublished paper.

[8] D. Salzmann, *Atomic Physics in Hot Plasmas* (Oxford University Press, Oxford, 1998) pp. 77–82, beginning of Chapter "Atomic Processes in Hot Plasmas".

[9] J. Bauche, C. Bauche-Arnoult, and O. Peyrusse, in *Atomic Properties in Hot Plasmas: From Levels to Superconfigurations* (Springer, 2015) Chap. 6, pp. 176–182.

[10] J. Bauche, C. Bauche-Arnoult, and O. Peyrusse, Journal of Quantitative Spectroscopy and Radiative Transfer **99**, 55 (2006), radiative Properties of Hot Dense Matter.

[11] J. Bauche, C. Bauche-Arnoult, and O. Peyrusse, in *Atomic Properties in Hot Plasmas: From Levels to Superconfigurations* (Springer, 2015) Chap. 6, pp. 161–165.

[12] C. Bowen, Journal of Quantitative Spectroscopy and Radiative Transfer **71**, 201 (2001), radiative Properties of Hot Dense Matter.

[13] R. D. Cowan, *The theory of atomic structure and spectra*, Vol. 3 (Univ of California Press, 2023) p. 404.

[14] J. Bauche and C. Bauche-Arnoult, Journal of Physics B: Atomic, Molecular and Optical Physics **33**, L283 (2000).

[15] K. Fournier, J. Bauche, and C. Bauche-Arnoult, Journal of Physics B: Atomic, Molecular and Optical Physics **33**, 4891 (2000).

[16] M. Busquet, Journal of Quantitative Spectroscopy and Radiative Transfer **99**, 131 (2006), radiative Properties of Hot Dense Matter.

[17] H. Van Regemorter, Astrophysical Journal, vol. 136, p. 906 **136**, 906 (1962).

[18] V. P. Shevelko, *Atoms and their spectroscopic properties*, Vol. 18 (Springer Science & Business Media, 1997) pp. 141–149.

[19] J. Davis, Journal of Quantitative Spectroscopy and Radiative Transfer **14**, 549 (1973).

[20] "Effective Nuclear Charge," (2025), [Online; accessed 2025-08-22].

A Code

To obtain the plots in the results section, the relevant equations were implemented in Python using the Matplotlib library. The code is organized into several files:

- `atomic_model.py`: Contains functions for the different key equations in order to answer the research questions related to the atomic model.
- `question_1.py`: Contains functions to analyze how the reduced normalized populations depend on excitation energy, electron temperature and density.
- `question_2.py`: Contains functions to analyze the different models of the effective temperatures.
- `question_3.py`: Contains functions to analyze the different models of the Gaunt factor.

The complete code listings can be found in this GitHub repository.